High Entropy Alloys III

High-Throughput Synthesis and Characterization of Thin Film High Entropy Alloys Based on the Fe-Ni-Co-Cu-Ga System

Samuel Guérin[1]; Anaïs Guyomarc'h[1]; Brian Hayden[1]; Sergey Yakvolev[1]; James Cotton[2]

1. Ilika Technologies Ltd. Kenneth Dibben House, University of Southampton Science Park, Chilworth, Southampton, SO16 7NS, United Kingdom
2. The Boeing Company, Metallic Materials Group, PO Box 3707, MC 19-HP, Seattle, WA, USA 98124-2207

Abstract

High entropy alloys offer a new approach in alloy design by combining multiple elements around equiatomic proportions; relatively simple crystal structures may be obtained and promising properties have been reported. However, there is a major challenge to validate complex phase equilibria predictions for such multifold chemistries, and subsequently, to optimize composition within a selected alloy system. In the present case, high-throughput techniques were employed for the synthesis and characterization of thin films of varying composition around the equiatomic FeNiCoCuGa composition. Continuous thin films were deposited by modified molecular beam epitaxy (MBE) technology and annealed in a reducing atmosphere. Subsequently, the thin films were characterized by EDS, SEM and XRD. The results allow isothermal and isochemical sections of the quinary phase diagram to be drawn, revealing domains of three disordered crystalline phases, as well as mapping of their relative concentrations. General trends of the effect of the constituent elements on the phase concentrations and domain of existence can easily be accessed. These results are compared with data obtained from bulk samples.

Introduction

High entropy alloys (HEA) have been the subject of numerous publications in the past 10 years [1-3] as mixing of more than 4 individual components around equiatomic compositions often results in the formation of only one or two disordered crystalline phases. This relatively new field of research deviates strongly from the common research approach of introducing low level additions to an already well-established system with a view to improve the properties of a single phase material. Conventional methods to study metallic alloys usually require synthesis of multiple samples, which limits the number of compositions to be reasonably investigated within a given time frame, and thus, limiting the ability to understand properly the relations between the equilibrium phases and composition. High-throughput technologies using thin films have been developed to allow the synthesis of large compositional spreads on a single substrate [4]. These offer significant advantages which can improve and accelerate research into a myriad of engineering materials. The main issue of

high-throughput techniques via thin films is whether the results obtained on thin films are transferrable to results obtained on standard bulk samples.

Experimental

Thin film samples were deposited onto silicon coated with silicon nitride substrates using a High-Throughput Physical Vapor Deposition (HT-PVD) apparatus [4] at a substrate temperature of 150 °C. The base pressure in the deposition tool was around $2x10^{-9}$ Torr and the elements were evaporated using either electron beam sources (for Ni, Fe and Co) or effusion cells (for Ga and Cu). Following deposition the thin films were taken out of vacuum and characterized for composition (by energy dispersive spectroscopy (EDS), using either a JEOL 5910 SEM equipped with an Oxford Instrument Inca 300 EDS detector or a Tescan Vega 3 SEM equipped with an Oxford Instruments X-Max EDS detector) and crystal structure (by XRD using a Bruker D8 diffractometer equipped with a Hi-Star GADDS 2D detector). The samples were subsequently annealed in a mixture of 5% H_2 in Ar at 700 °C for 30 mins (ramp rate of 5 °C/s) using a Lenton tube furnace. Characterization of the annealed specimens was then repeated using EDS and XRD. Typically, the EDS spectra were collected using a 3x3 macro spanning 26 mm and the data were interpolated to a 14x14 macro spanning 26 mm. The XRD data was acquired as a 7x7 macro for the as-deposited samples and as a 14x14 macro for the samples following annealing; both macro covered a 26 x 26 mm^2 area. The thickness of the thin films used for XRD varied within each sample between 150 and 200 nm and the films were well-adhered to the substrate with minimal interfacial reaction.

Results and Discussion

Because thin film deposition takes place essentially in two dimensions, the compositional degrees of freedom permissible in any arbitrary chemistry are analogous to projecting multi-component phase diagrams, (n-1), where n is the total number of components. Hence, complete binary compositions are permissible, as are ternary compositions because the sum elemental percentages total 100%. In the case of a quinary system, the two additional degrees of freedom must be accommodated via additional deposits and the results integrated computationally. To remedy this problem, we have decided to allow compositional variations of the three ferromagnetic elements (Fe, Ni and Co) across a single substrate and to introduce the other two elements at constant levels across one sample. Therefore, a series of 11 samples were synthesized in which the Fe, Ni and Co variations were kept constant while the relative amounts of Cu and Ga were varied, thus allowing a more systematic mapping of all the possible compositions. For this series, two trends were necessary, one where the Cu and Ga content both increase concurrently from one sample to the other, and one where the Cu decreases whilst the Ga increases. The result is the list of samples shown in Table 1; it can be seen that the variations in Fe, Ni and Co remains similar between samples and centered around the equiatomic point whilst the Ga and Cu are varied between samples (classified as Low, Medium and High levels) but remain more or less constant within each sample (apart from changes induced by thickness variations of the thin film). An example of the relative

compositional variations is shown in Figure 1. This approach also enabled to visualize the data produced as a 2D plot of ternary diagrams as shown in Figure 3. In this representation the axis for Cu and Ga are merely indicative of the relative increases and actual atomic percentages can be found in Table 1.

Table 1: Summary of compositional spread covered by 9 samples of interest. Values in at%. The Ga and Cu concentrations have been classed as low (L, < 15 at%) in yellow, medium (M, 15 < < 25 at%) in green and high (H, > 25 at%) in blue.

	Fe		Ni		Co		Ga		Cu	
sample #	min	max	min	max	min	max	min	max	min	max
12640	19.7	52.8	0.6	35.6	6.4	50.5	7.9	12.5	8.3	12.2
12564	7.3	29.8	6.8	38.4	7.5	29.4	11.6	14.8	19.3	25.1
12561	6.3	31.5	4.7	35.3	6.6	25.7	10.4	13.9	26.1	34.4
12555	6.4	33.9	7.5	36.4	5.6	38.5	16.6	21	10.5	13.2
12568	8	28.1	2.9	32	8.9	28.5	19.9	24.8	18.4	24.3
12575	6	27.9	4	28.1	7.6	24.5	17.4	22.3	26.9	34.9
12580	5.4	26.5	6.7	36.1	6.3	25.2	28.6	32.9	10.7	13.9
12557	4.8	22.4	9.4	28.8	4.6	25	23	26.4	21.6	25.2
12579	6.3	32.6	0	21.1	6.4	27.4	26.1	33	22.4	29.5

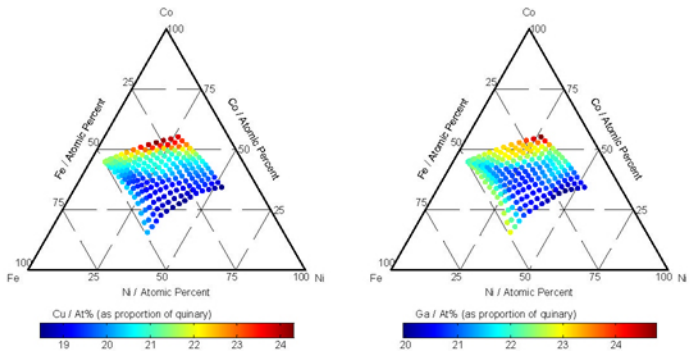

Figure 1: Concentrations of Cu (left) and Ga (right) for sample #12568 as a function of the ternary space of FeNiCo covered by a single sample. The observed variations in Cu and Ga are a direct reflection of variations in thickness across the sample.

Co-deposition of the five constituent elements on silicon nitride resulted in very smooth films with a mirror like surface and no discernible features or variation which were attributed to variation in composition. XRD collected on the as-deposited samples revealed a partially crystallized material, with peaks corresponding to a mixture of one fcc and one bcc phases. Annealing was accomplished using a reducing mixture of hydrogen in argon in order to reduce the risk of oxide formation. Furthermore, the samples were all deposited on silicon nitride coated silicon substrates as the silicon nitride offers an inert layer which discourages

silicide formation. The composition of the thin films was verified following the annealing and no deviation above the random measurement error was observed.

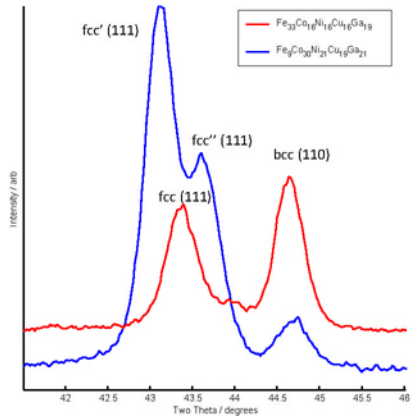

Figure 2: Diffractograms from two compositions of FeCoNiCuGa after annealing to 700 °C in 5% H_2 in Ar. It shows the existence and broad position of three fcc phases (the one labelled fcc splits in fcc' and fcc'') and one bcc phase.

Following annealing, the samples changed in appearance from highly reflective silvery metallic to a duller metallic layer, indicative of an increase in surface roughness caused by the annealing process. The thin films were characterized once more by XRD. This time the thin films appeared well crystallized with full width at half maximum peak values below 0.4°. A good level of crystallinity was observed throughout the compositional space investigated. Similarly to the as-deposited samples, only bcc and fcc phases were observed, however the fcc observed in the as-deposited samples split in two fccs for iron poor regions. Figure 2 shows examples of the three main reflections observed across the entire FeNiCoCuGa system. Throughout the compositional spread covered we observed the following mixtures of phases: fcc on its own, bcc on its own, fcc and bcc, fcc' and fcc'', fcc' and fcc'' and bcc. It also appears that fcc splits into fcc' and fcc'', since for certain compositions, both fcc' and fcc'' always coexist and fcc is never observed with either fcc' and fcc''. Using the grouping observed we have been able to produce a schematic phase diagram for the FeNiCoCuGa system after annealing to 700 °C as shown in Figure 3. From this figure it can be seen that pure single phases are only found for low copper content with a large region of pure fcc for the iron poor region of sample corresponding to low Cu and low Ga and a sample made mostly of pure bcc obtained for low copper level and high Ga content. The other samples were all displaying a mixture of either 2 phases or 3 phases. In general the bcc phase becomes more predominant for Fe rich compositions; this can be linked to the fact that pure iron is the only element out of the five elements under consideration which possesses a stable bcc structure. The split of fcc into fcc' and fcc'' only happens for low Fe levels and can also be seen to shift towards Fe poorer compositions as the Ga content

increases and shifts out of the range of compositions under investigation for the sample with high copper and high gallium. Increasing the copper levels above the "low" level does not seem to be associated with any marked variations in the phases observed or their domain of existence. Higher Ga levels appear to stabilize the bcc phase, which is interesting given that Ga does not occur in this structure under standard conditions.

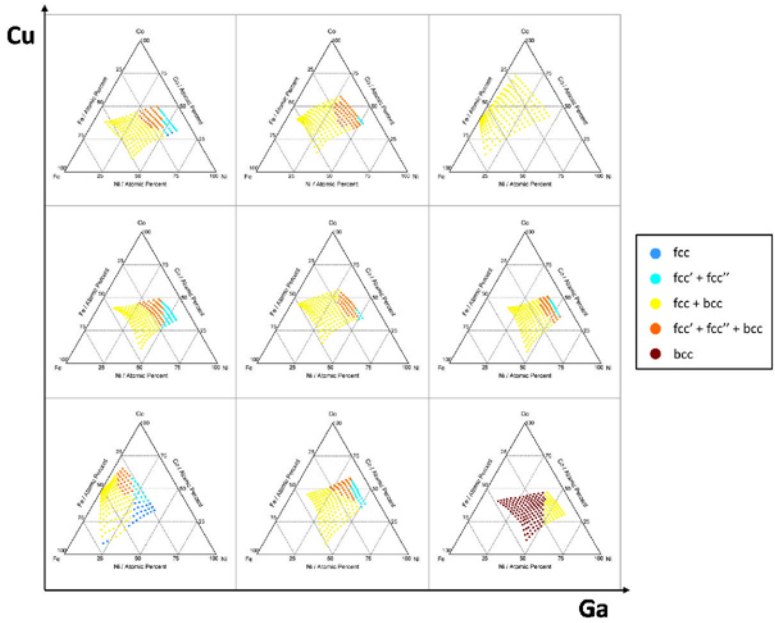

Figure 3: Schematic phase diagram for the FeNiCoCuGa system after annealing to 700°C

Having established some basic observations about the different phases and their domain of existence, further examination of the low copper region reveals more details about the trends observed. This is illustrated in Figure 4 where two additional samples are used to map the phases present. This time the split of the fcc phase into fcc' and fcc'' only happens in the samples with relatively high Cu and low to medium levels of Ga. The split is also still linked to regions with low Fe concentrations. Pure bcc phase is still only found for the high Ga content, spreading from Fe rich compositions as the Ga content increases. Sample #12566 reveals that a pure bcc phase was obtained for the whole FeNiCo compositional spread covered when a very high Ga level was used.

Using these observations and groupings, the entire XRD dataset collected (2156 diffractograms from 11 samples) was analyzed by peak fitting pseudo-Voigt curves in order to accurately map peak intensities, peak positions, peak areas and full width at half maximum of the 4 phases. The peak areas were then used to estimate the relative percentages of each phase within the compositional spread covered. In general the concentrations of the phases

are found to follow the observations about their domain of existence. However finer analysis reveal that the concentration of the bcc phase is primarily linked to Ni poor compositions. The fcc phase follows the opposite behavior with the highest concentrations linked with the Ni rich compositions. The maps of peak position reveal that the lattice parameter of the bcc phase does not vary greatly apart from the samples with relatively high gallium content where its domain of existence also increases. The lattice parameter of the fcc phase does display more variations with a shift towards smaller unit cells for increasing Ni concentration and a general increase in lattice parameter for increasing Ga concentration. The variation in Cu concentration seems to have limited effect on the lattice parameter of the fcc phase which fits with previous comments. This would imply that there is limited solubility or effect due to Cu within the quinary system investigated.

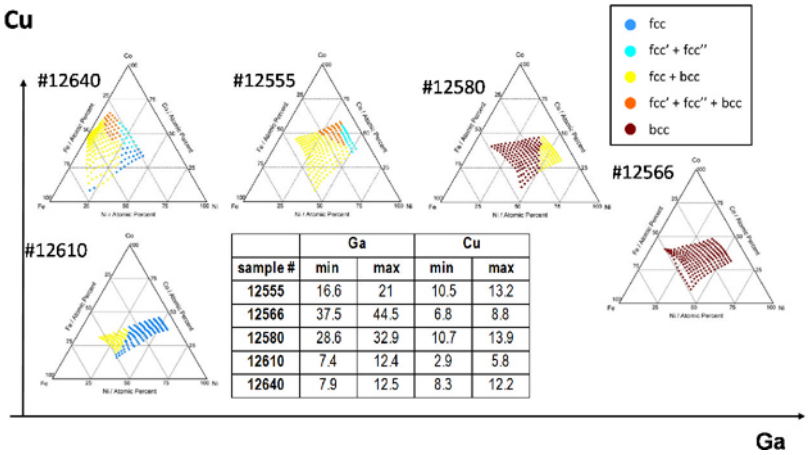

	Ga		Cu	
sample #	min	max	min	max
12555	16.6	21	10.5	13.2
12566	37.5	44.5	6.8	8.8
12580	28.6	32.9	10.7	13.9
12610	7.4	12.4	2.9	5.8
12640	7.9	12.5	8.3	12.2

Figure 4: Schematic phase diagram for the FeNiCoCuGa system after annealing to 700 °C, maps concentrating on the low Cu region. The inserted table lists the at.% of Cu and Ga of each sample with respect to the quinary system.

Due to the observations stated above and the change in appearance of the thin films upon annealing, SEM studies were carried out to help understand the XRD results. Figure 5 shows secondary electron images obtained at a magnification of 50,000X on a single location on each of nine selected samples. The evaluation location was chosen to be closest to the Fe-Ni-Co equiatomic composition within each sample. The phases observed by XRD at each location are noted on each image. The SEI images clearly show the presence of submicron grains. These grains are only present in the annealed samples; the as-deposited samples were smooth with no discernable features. The features appear less pronounced for Ga-rich compositions but are still clearly present; in addition to the grains, there appear to be smaller (<100 nm) white particles on the surface which are more prominent for Ga-rich region. Interestingly, the grains observed are larger than the film thickness (grains around 500 nm and thickness of 200 nm at most). Due to the choice of the location within each sample, no investigation of the effect of varying the FeNiCo content was attempted.

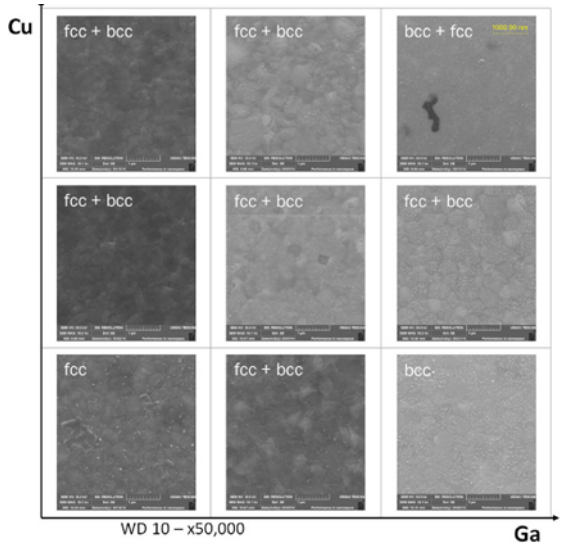

Figure 5: SEM Secondary Electron Images of 9 locations on 9 samples of the FeNiCoCuGa system after annealing to 700°C. The locations were the closest to the equiatomic composition within each sample. Acquired at 30 kV and x50,000 magnification. Scale bar is one micron.

EDS mapping was carried out on these same locations and distinct groupings of elements were observed following annealing for most samples apart from one. Using in-house software, we could determine which elements were correlated together by mapping the distribution of intensities on each pixel. Figure 6 gives a representation of this distribution across the composition range. The segregation observed does not match the grains imaged by SEM and shown in Figure 5. The grouping of elements clearly varies as a function of the Cu and Ga levels. The present study did not investigate the variations due to Fe, Ni or Co but only the variations due to Cu and Ga. The sample with low Cu and low Ga appear to not have segregated at the resolution used. For relatively low Ga levels and medium Ga with low Cu, Ni, Ga and Cu appear to segregate together as well as Fe and Co. Increasing the Ga level and for medium to high concentration of copper, the copper segregates separately, the Fe and Co together and the Ni and Ga together. Finally for high Ga levels, the copper still segregates on its own whilst the remaining 4 elements stay grouped.

A clear benefit of the high-throughput approach to study these materials is the large amount of data generated in a relatively quick time-span. This data can be used to refine theoretical modelling approach by providing experimental data to strengthen the calculations. However correlation between the thin film data and data obtained from bulk samples is needed. In this system, bulk samples of nominal composition $Fe_{20}Co_{20}Ni_{20}Cu_{20}Ga_{20}$ were prepared by arc melting and casting. XRD reveals the co-existence of an fcc phase with a bcc phase, consistent with the result obtained from the thin film for a similar composition.

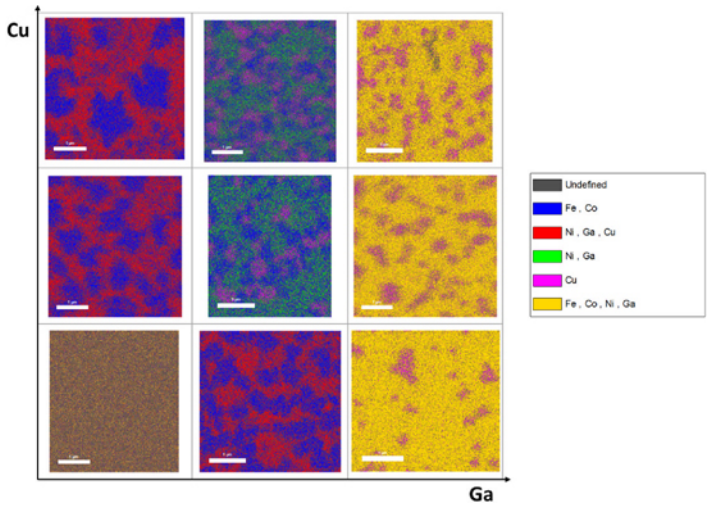

Figure 6: Representation of the distribution of grouping of elements deduced from EDS mapping of 9 locations on 9 samples of the FeNiCoCuGa system after annealing to 700°C. The locations were the closest to the equiatomic composition within each sample. Scale bar is one micron.

Conclusions

We have shown that high-throughput synthesis and characterization of thin film alloys may correlate well to bulk data in terms of phase stability, and with considerably greater latitude. It allows a rapid screening of a system of interest to assist in compositional downselection. It also offers access to large amount of experimental data which may be applied to computational thermodynamic and microstructural development models. Future work will focus on mechanical properties of the material using nanoindentation with a view to expanding the viability of high-throughput thin films alloys to metallic alloy research.

References

[1]. J-W Yeh et al., "Nanostructured High-Entropy Alloys with Multiple Principal Elements: Novel Alloy design Concepts and Outcomes", *Advanced Engineering Materials*, 6 (2004), 299.

[2]. Y Zhang, Y Zhou, "Solid Solution Formation Criteria for High Entropy Alloys", *Materials Science Forum*, 561-565 (2007), 1337

[3]. D B Miracle et al. "Exploration and Development of High Entropy Alloys for Structural Applications", *Entropy*, 16 (2014), 494

[4]. S Guerin, B E Hayden, "Physical Vapor Deposition Method for the High-Throughput Synthesis of Solid-State Material Libraries", *Journal of Combinatorial Chemistry*, 8 (2006) 66